Supplementary Materials

$Nd_{2-x}Sr_xNiO_4$ Solid Solutions: Synthesis, Structure and Enhanced Catalytic Properties of Their Reduction Products in the Dry Reforming of Methane

Oleg A. Shlyakhtin [1,*], Grigoriy M. Timofeev [1], Sergey A. Malyshev [1,2], Alexey S. Loktev [3,4,5], Galina N. Mazo [1],
Tatiana Shatalova [1,2,6], Veronika Arkhipova [4], Ilya V. Roslyakov [5,6] and Alexey G. Dedov [3,4,5]

[1] Department of Chemistry, M.V. Lomonosov Moscow State University, 119991 Moscow, Russia
[2] Department of Materials Sciences, Shenzhen MSU-BIT University, Shenzhen 518172, China
[3] A.V. Topchiev Institute of Petrochemical Synthesis, Russian Academy of Sciences, 119991 Moscow, Russia
[4] Department of General and Applied Chemistry, Gubkin Russian State University of Oil and Gas, 119991 Moscow, Russia
[5] N.S. Kurnakov Institute of General and Inorganic Chemistry, Russian Academy of Sciences, 119991 Moscow, Russia
[6] Department of Materials Sciences, M.V. Lomonosov Moscow State University, 119991 Moscow, Russia
* Correspondence: oleg@inorg.chem.msu.ru

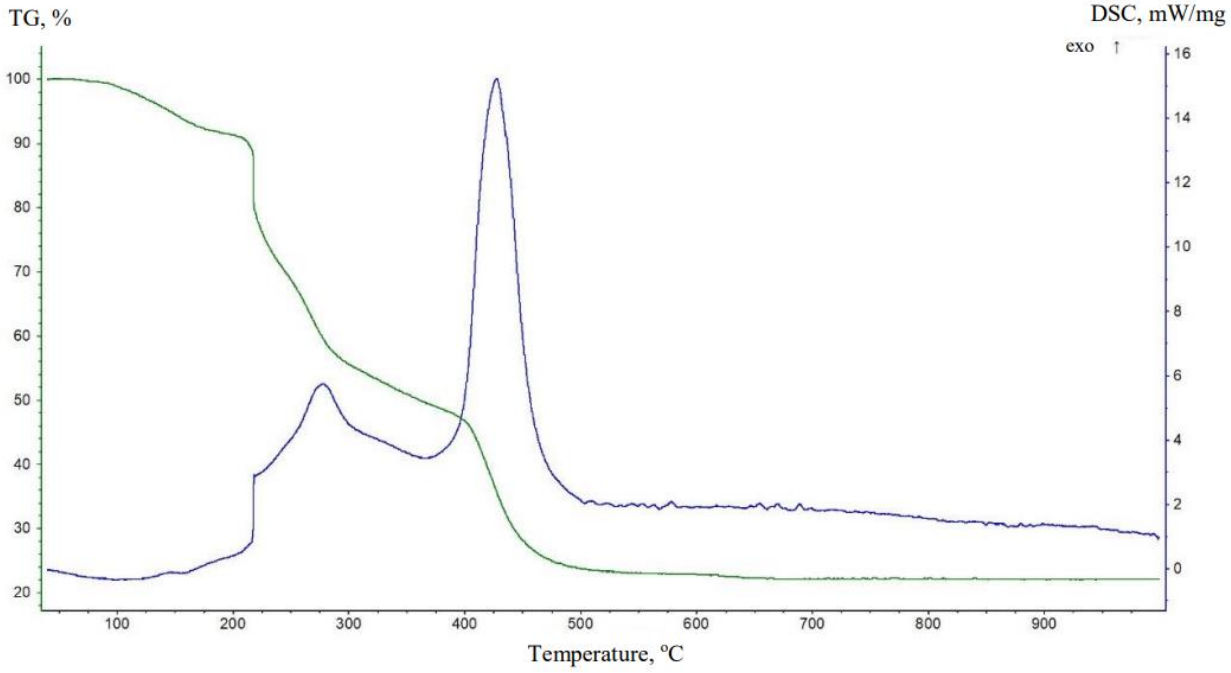

Figure. S1. TG (green) and DSC (blue) profiles of freeze-dried Nd_2NiO_4 precursor.

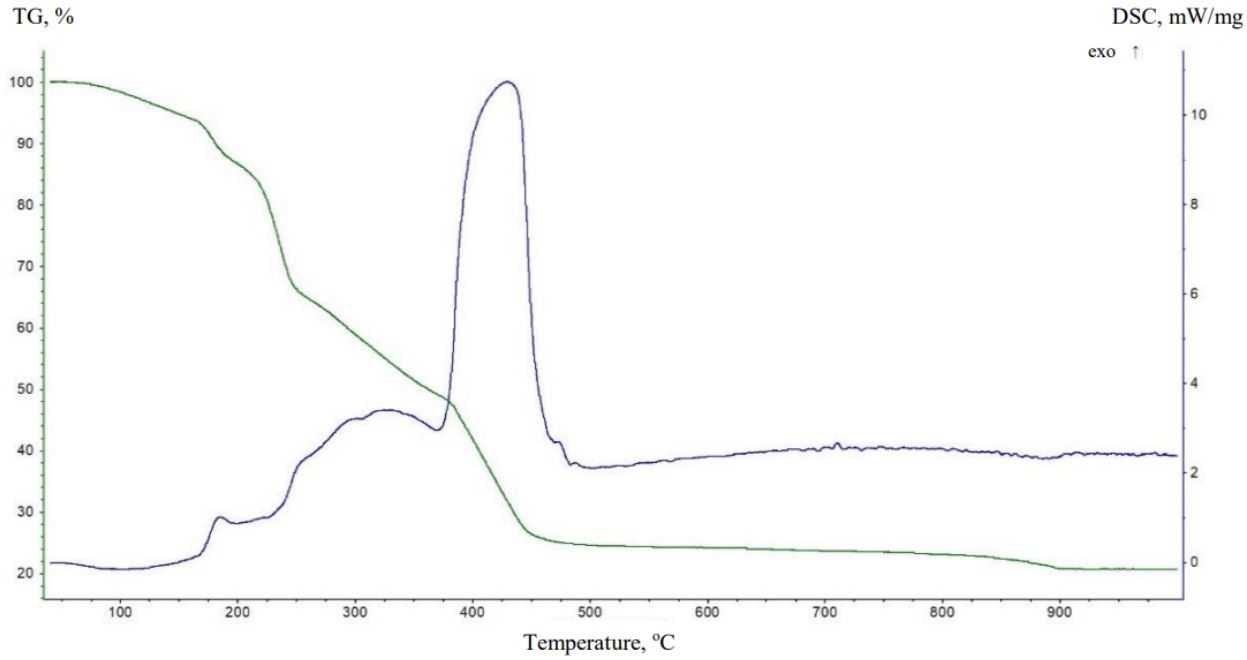

Figure. S2. TG (green) and DSC (blue) profiles of freeze-dried $Nd_{0.6}Sr_{1.4}NiO_4$ precursor.

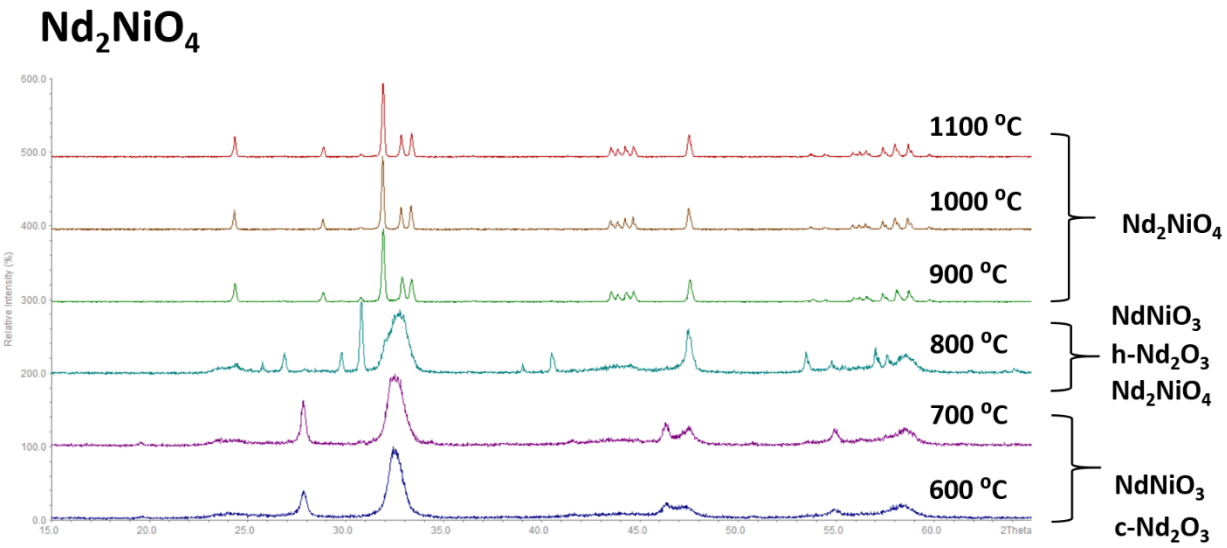

Figure. S3. XRD patterns of thermal decomposition products of Nd_2NiO_4 (x=0) precursors at different temperatures.

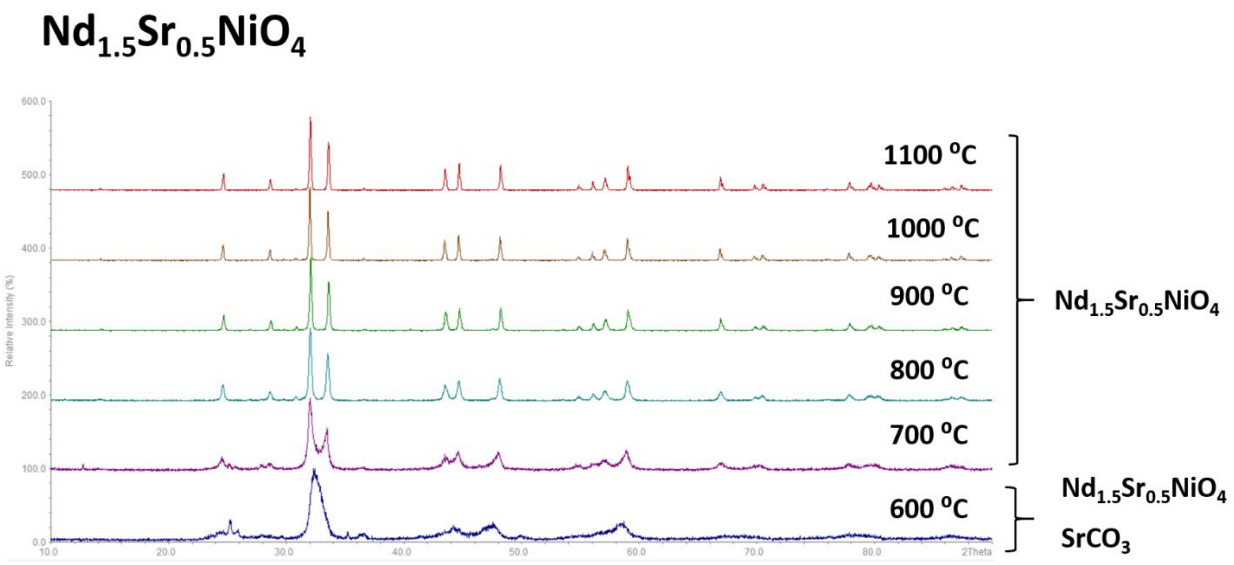

Figure. S4. XRD patterns of thermal decomposition products of $Nd_{1.5}Sr_{0.5}NiO_4$ (x=0.5) precursors at different temperatures.

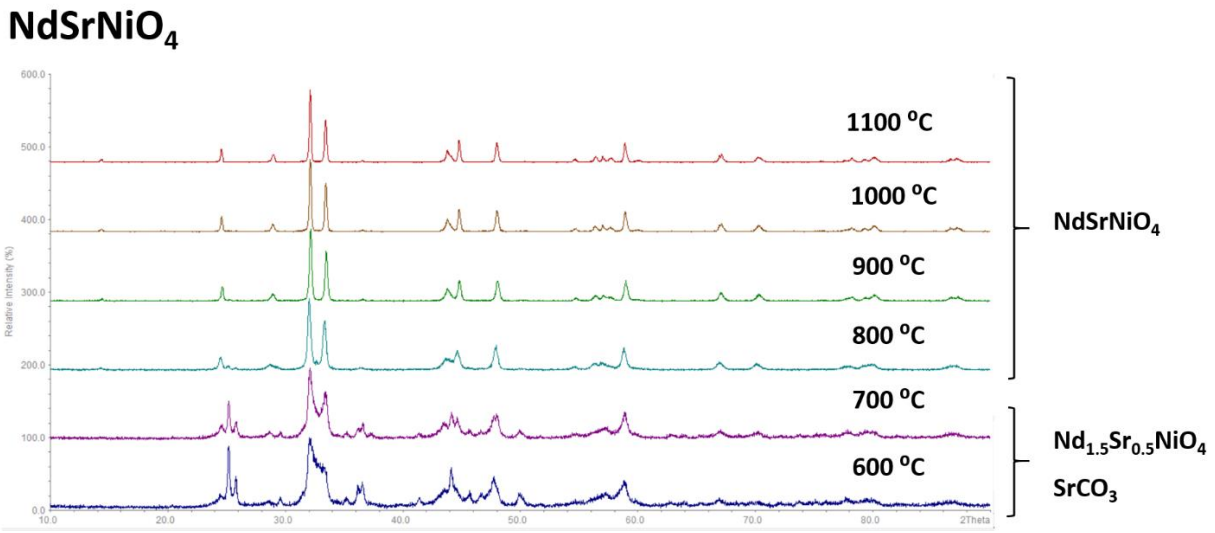

Figure. S5. XRD patterns of thermal decomposition products of $NdSrNiO_4$ (x=1) precursors at different temperatures.

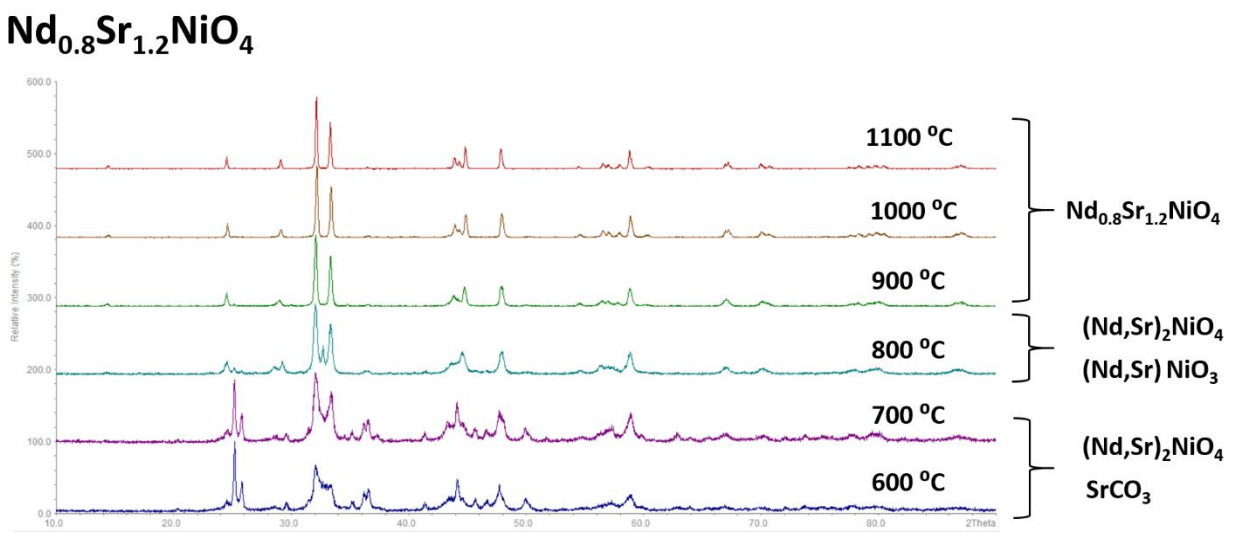

Figure. S6. XRD patterns of thermal decomposition products of $Nd_{0.8}Sr_{1.2}NiO_4$ (x=1.2) precursors at different temperatures.

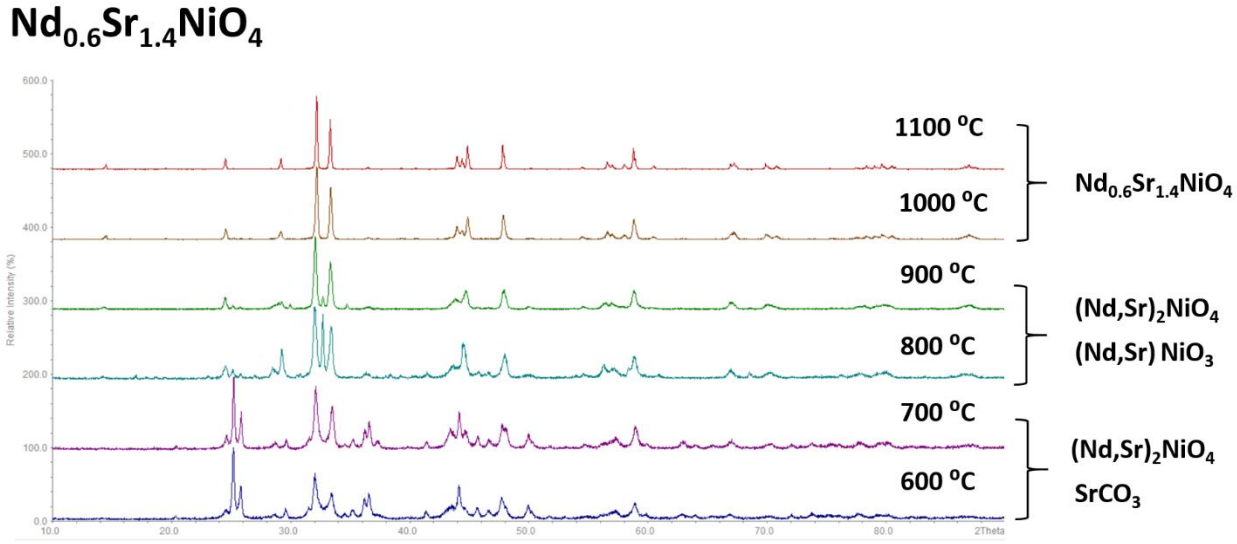

Figure. S7. XRD patterns of thermal decomposition products of $Nd_{0.6}Sr_{1.4}NiO_4$ (x=1.4) precursors at different temperatures.

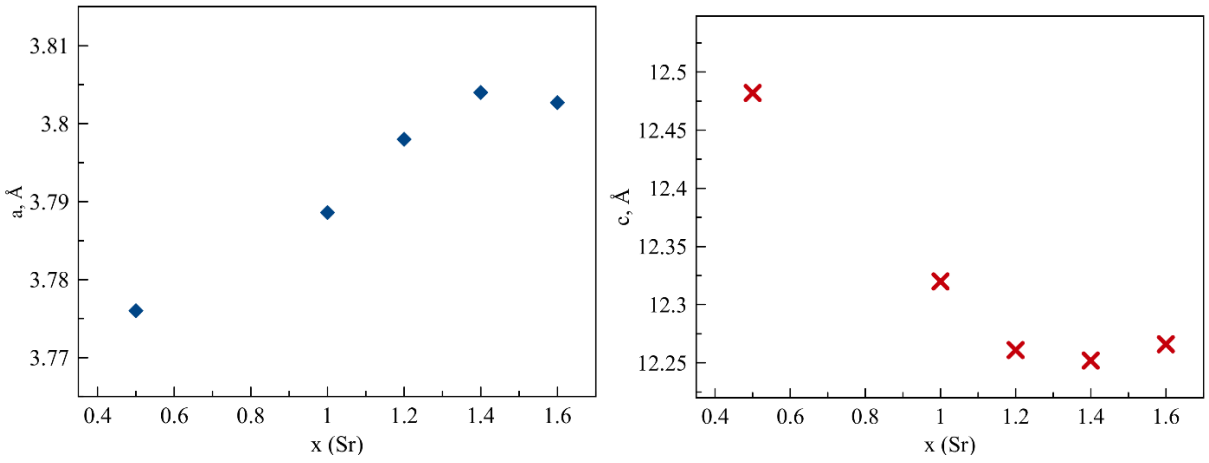

Figure. S8. The dependence of $Nd_{2-x}Sr_xNiO_{4\pm\delta}$ lattice parameters on Sr content.

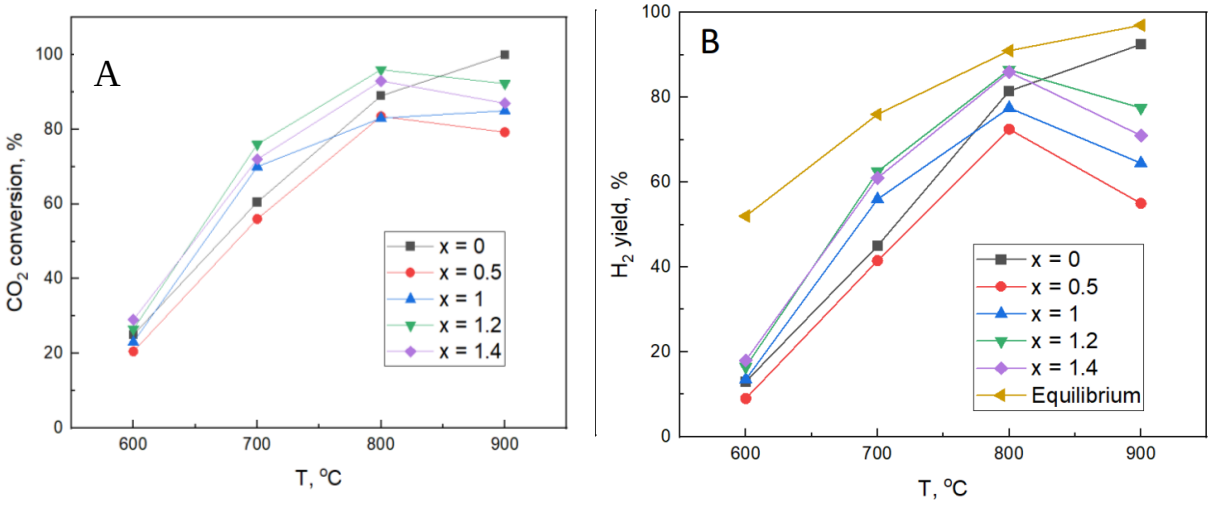

Figure. S9. CO_2 conversion (A) and H_2 yield (B) over the reduction products of various composites. The calculated values of H_2 yield are given according to [13, 31–33]

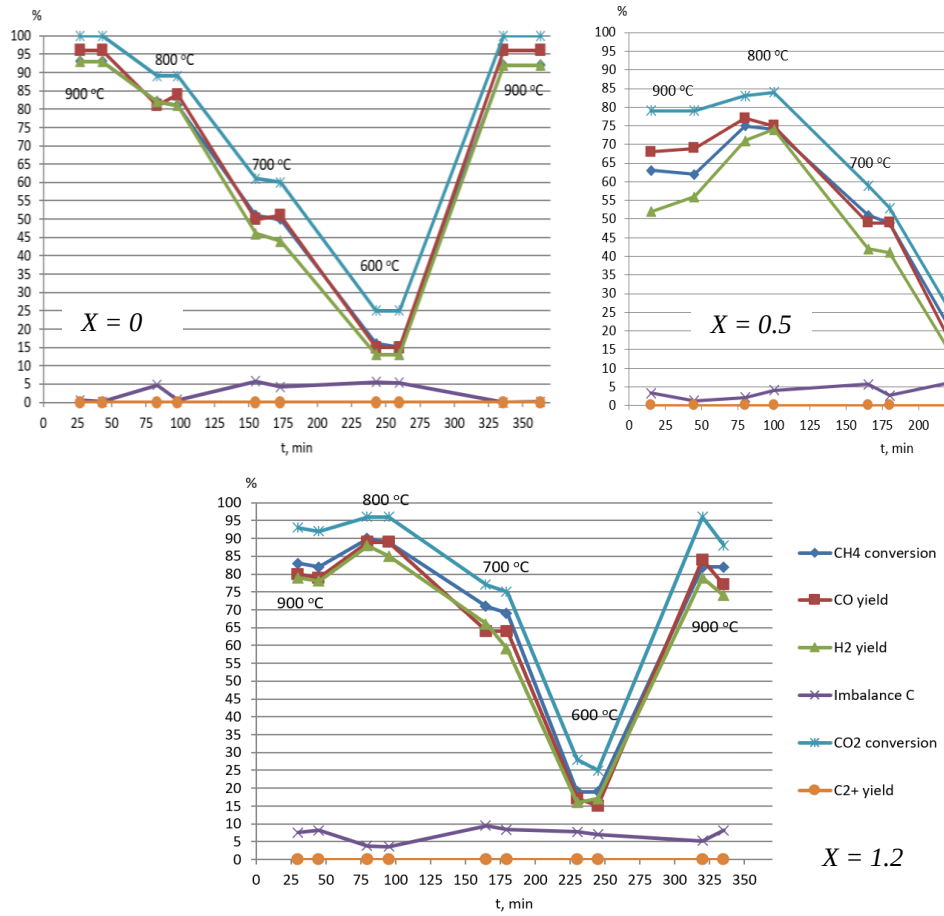

Figure. S10. The results of testing the composites with various Sr content in the DRM process.

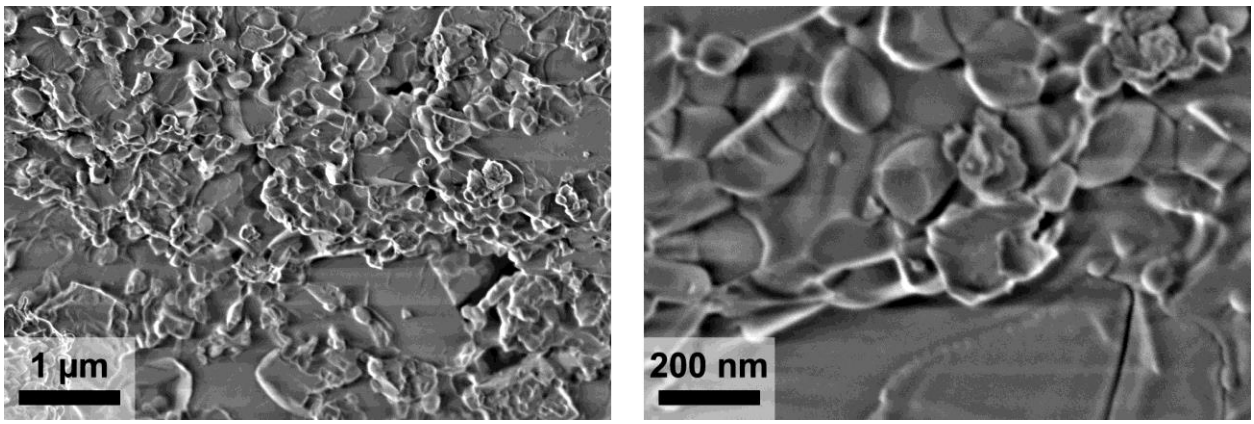

Figure. S11. SEM micrographs of the spent catalyst (x = 1.4).